AD-A189 317 RELATIONSHIPS BETWEEN REMOTELY-SENSED SURFACE PROPERTIES AND SUBSURFACE STRUCTURE IN THE OCEAN(U) NAVAL OCEAN SYSTEMS CENTER SAN DIEGO CA P C FIEDLER

1/1

UNCLASSIFIED 06 JAN 88 F/G 8/3 NL

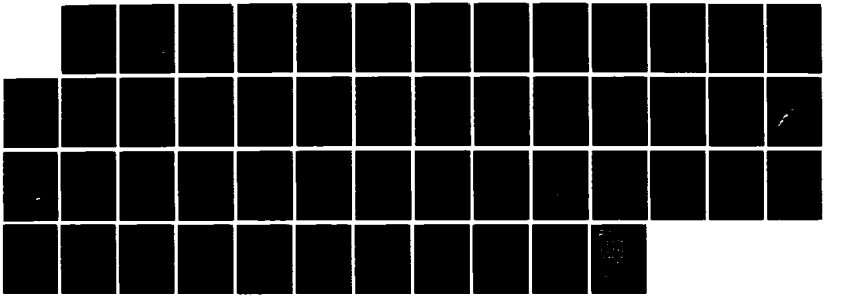

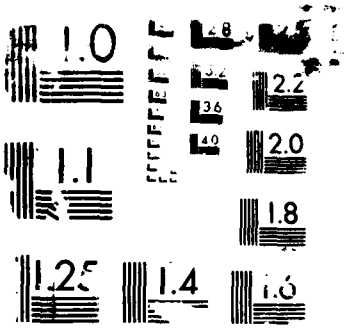
1.0
1.1
1.25
1.4
1.6
1.8
2.0
2.2
36
40

RELATIONSHIPS BETWEEN REMOTELY-SENSED SURFACE PROPERTIES AND SUBSURFACE STRUCTURE IN THE OCEAN

ASEE/ONT Postdoctoral Fellowship - Final Report

Paul C. Fiedler
Naval Ocean Systems Center

6 January 1988

The objective of my fellowship study was to assess relationships between remotely-sensed surface variables and subsurface structure in the ocean. Subsurface thermal structure is very important in Navy operations involving acoustic detection of underwater targets. It is also of fundamental importance for both research and monitoring of oceanic mixing and productivity.

Remote sensing is an appealing alternative for oceanographers who have spent weeks on a rolling ship doing repetitive station sampling. Unfortunately, a sensor on an aircraft or satellite receives little or no electromagnetic signal from the water column below the surface. Infrared radiation is attenuated within less than a millimeter and visible radiation within meters, or tens of meters in the clearest oceanic water. Does this mean that the subsurface water column is inaccessible to remote sensors? Not if subsurface variables are correlated with remotely sensed variables like infrared brightness temperature or upwelled visible radiance. However, remote sensors cannot be fully exploited until we know how much information about subsurface patterns and structure is contained in a surface signal.

This final report consists of three parts. First, a statistical analysis of historical temperature-depth data from the California Current, recently accepted for publication in Journal of Geophysical Research. Second, an analysis of temperature and color data from ship and satellite as predictors of vertical structure (from XBT data) in the Gulf of California. Finally, a description of a vertical model of the ocean surface layer developed to explore surface-subsurface relationships and the underlying physical and biological processes.

Part I. Surface Manifestations of Subsurface Thermal Structure in the California Current

ABSTRACT

Remote sensing is useful for studying certain oceanographic problems only if the signal obtained from the sea surface contains information about subsurface structure. Historical bottle temperature data from the California Current were analyzed for surface manifestations of vertical structure and subsurface mesoscale structure. Results showed that surface temperature is useful in predicting thermocline strength over a large area south of Point Conception: the error of a regression estimate is 20-30% less than the error of the seasonal mean. However, surface temperature gives little useful information about mixed layer depth. Mesoscale patterns of temperature at the surface and at depth -- caused by eddies, meanders and upwelling -- are coherent ($r^2>0.50$) to a depth below the mixed layer only off central California and Point Conception and along the coast of Baja California. Coherence is most likely to extend below the mixed layer during summer, when the water column is strongly stratified and the mixed layer is most shallow. Thus, some aspects of subsurface structure, within limited regions of the California Current, have surface manifestations potentially detectable by satellite sensors.

1. INTRODUCTION

Satellite sensors have revolutionized oceanography in the past decade by providing repetitive and synoptic measurements of temperature, color, winds, and currents over large areas of the sea surface. Sea-truth validation of satellite estimates of surface parameters has led to sensor and algorithm refinements that have reduced errors to acceptable levels for many applications. However, for studies of structure and processes below the sea surface, even error-free satellite data are useful only if the surface signal contains information about subsurface structure. For example, in an XBT survey across the central north Atlantic (Dugan 1980), an unambiguous surface temperature signal was detected for only one of four cold-core eddies observed in the permanent thermocline. A thermocline front had no corresponding surface temperature signal, while a surface thermal front did not extend into the thermocline. From a global survey of SST fronts detected by satellite, Legeckis (1978) concluded that isothermal surface layers obscure subsurface horizontal temperature gradients in tropical oceans year-round and in subtropical oceans during summer.

Satellite infrared temperature data have been used increasingly in studies of the California Current System as the importance of mesoscale variability has become more apparent (Bernstein et al. 1976, Koblinsky et al. 1984, Flament et al. 1985). Above 500m, this system consists of (1) a broad, equatorward California Current with a low-salinity core about 400 km

offshore, (2) a poleward California Undercurrent with a core at ~300m depth over the continental slope, and (3) a fall-winter, poleward California Countercurrent at the surface within 150 km of the coast (Simpson et al. 1986). Mesoscale coastal jets or streamers and offshore eddies are much more energetic than the large-scale mean surface flows, as is generally true in eastern boundary currents (Wyrtki et al. 1976).

The California Cooperative Oceanic Fisheries Investigations (CalCOFI) program has sampled standard depths at stations covering most of the California Current System since 1950 (Fig. I-1). Gross vertical structure parameters such as mixed layer depth, thermocline depth, and stratification or stability can be derived from CalCOFI temperature data. Although the 37-74 km spacing of CalCOFI stations may barely resolve mesoscale eddies, meanders in the core of the California Current, and coastal upwelling, such features are clearly visible in maps of cruise data (see Wyllie 1966 and CalCOFI Data Reports).

In this paper, I analyze a large set of CalCOFI hydrographic data to answer two basic questions about the utility of remotely sensed surface data in the California Current:

(1) Can information about vertical structure below the surface be derived from surface temperature?

(2) Are mesoscale patterns of surface temperature coherent with patterns below the mixed layer or thermocline?

Surface data will be considered useful in estimating subsurface structure (Question #1) if they can produce an estimate that is more precise than an estimate based on climatology alone (i.e. if the standard error of the regression estimate is less than the standard deviation around annual or seasonal station means). Vertical coherence of mesoscale patterns (Question #2) was examined within regions with dimensions of 100-400 km to exclude larger-scale latitudinal and onshore-offshore patterns. Variability of temperature at standard depths within regions represents effects of offshore eddies, California Current meanders, coastal upwelling, and other structures and processes resolved by the station grid. Correlation between the surface and depth is a measure of the coherence of mesoscale surface structure with depth. Alternatively, it is a measure of the contribution of subsurface structure to the surface temperature signal.

The practical utility of estimates of subsurface structure derived from surface observations will depend on the particular problem at hand. This empirical analysis is intended to explore the potential and limitations of extrapolating accurate remotely-sensed surface data into the water column. Errors introduced into the surface signal at the air-water interface, in the atmosphere, and by the sensor are not considered here.

2. METHODS

The CalCOFI data set includes temperature at fourteen standard depths (0, 10, 20, 30, 50, 75, 100, 125, 150, 200, 250, 300, 400, and 500m) from subsets of the basic station grid (Fig. I-1) occupied on 200 cruises from February 1950 to October 1984 (7-231 stations per cruise).

2.1. Vertical structure

Three vertical structure parameters were estimated from discrete temperature profiles. **Thermocline strength** ($|\Delta T/\Delta z|$) was calculated in the depth interval with the maximum vertical temperature gradient. Location of the **thermocline depth** within this interval was weighted by the temperature gradients above and below the interval. **Mixed layer depth** was calculated as the depth at which temperature extrapolated from the apparent thermocline equaled surface temperature (Wyrtki 1971). Thus, mixed layer depth is always less than the thermocline depth.

CalCOFI bottle samples cannot completely describe the vertical structure seen in continuous temperature profiles I-2). Thermocline strength is underestimated (e.g. Fig. I-2b). Fine-scale features such as steps and inversions are not resolved (Fig. I-2c,e). Mixed layer depth may be estimated accurately (Fig. I-2a,c) or not (Fig. I-2b). About 10% of the stations, for which the bottle data gave a mixed layer depth $\leq$ 0m (Fig. I-2d) or a thermocline in the deepest interval of the cast were considered to be inadequately described by bottle samples and

were omitted from the analysis.

Linear regression relationships between surface temperature and vertical structure parameters were calculated at 68 cardinal stations occupied >20 times (Fig. I-1). Utility of the relationships was measured by ratios of the rms error about the regression line to the standard deviation and to the mean of the dependent variable. The first ratio will be called the relative rms error. For large n, as in this analysis, the relative rms error is equal to the square root of the ratio of the residual sum of squares to the total sum of squares, or the square root of $(1 - r^2)$. The second ratio (rms error / mean) is a coefficient of error, or residual variation, analogous to the coefficient of variation.

2.2. Vertical coherence of mesoscale structure

Mesoscale regions are delimited in Figure I-1. The alongshore boundaries roughly define a transition zone between coastal and oceanic domains (Simpson et al. 1986). Regional correlations of temperature at 0m and at depth were calculated from sums of squares within cruises to eliminate variance and covariance between cruises (e.g. seasonal and interannual variability). Decorrelation depth is defined as the depth at which correlation with the surface equals 0.71 (r^2=0.50), calculated by linear interpolation between standard depths. Mean thermocline depth and mixed layer depth, as defined above, were calculated for each region and season. Differences between decorrelation depth and

mixed layer or thermocline depth were tested by the t-test (Sokal and Rohlf 1969) using the null hypothesis that r=0.71 at the mixed layer or thermocline depth.

3. RESULTS

3.1. Vertical structure

The mean mixed layer deepens and the thermocline weakens from nearshore to offshore stations (Fig. I-3). Mixed layer and thermocline depths are strongly correlated (Fig. I-4, r=0.933, n=6144). The step-like distribution of points in the scatterplot is an artifact of the discrete bottle spacing. Both features are most shallow nearshore between Pt. Conception and Pta. Eugenia and are correlated with thermocline strength (r=-0.34 for mixed layer depth and r=-0.43 for thermocline depth). The thermocline is strongest in two nearshore areas: the Southern California Bight and south of Pta. Eugenia.

Since mixed layer depth and thermocline depth are so closely related, only mixed layer depth and thermocline strength were considered as functions of surface temperature. Regressions of these two vertical structure parameters on surface temperature are summarized in Table I-1. Overall regression relationships are statistically significant ($P(r=0) << 0.001$ by the F-test, Fig. I-5). For both parameters, r^2 calculated within stations is greater than the overall value. R^2 calculated within stations and seasons is less than the overall value, perhaps due to small

ranges of the independent variable at some stations in some seasons.

Spatial patterns of relative rms error about the seasonal station regression lines are illustrated in Figure I-6. Regression on surface temperature gives an estimate of mixed layer depth with less error than that of the seasonal mean only in a small region offshore of Pta. Eugenia. Regression on surface temperature gives an estimate of thermocline strength with an error 20-30% less than that of the seasonal mean in a large area south of Point Conception. The coefficient of error (rms error / mean) of the estimates at these 50 southern stations is 0.34 ($\pm$0.27). North of Pt. Conception and at the offshore edge of the station grid, the regression estimate of thermocline strength is no more precise than the seasonal mean at a station.

3.2. Vertical coherence of mesoscale structure

Profiles of the correlation of surface temperature with temperature at depth in coastal, transition and oceanic regions are shown in Figure I-7. The decorrelation depth (r^2=0.50) is often significantly deeper than the mixed layer in regions off Central California and Pt. Conception and in coastal regions off BajaCalifornia (TableI-2). The decorrelation depth is most likely to be deeper than the mixed layer in summer, when the water column is strongly stratified and the mixed layer is most shallow. In contrast, the decorrelation depth tends to be significantly more shallow than the mixed layer in regions

offshore of Baja California, where the mixed layer is deepest. Among 15 regions and 4 seasons (60 cases), the decorrelation depth is deeper than the mixed layer in 26 cases ($r=0.83\pm.04$ at the mixed layer depth), not significantly different in 23 cases ($r=0.71\pm.04$), and more shallow in 11 cases ($r=0.55\pm.04$).

4. DISCUSSION AND CONCLUSIONS

4.1. Vertical structure

Mixed layer depth cannot be derived from surface temperature by linear regression in the CalCOFI data set; the deepest mixed layers are found at stations with intermediate surface temperatures (Fig. I-5). Shoaling of the thermocline can be correlated with either an increase or decrease in surface temperature by (1) seasonal warming and stratification of the surface layer or (2) upwelling of colder, deeper water caused by offshore transport of warm surface water. In either case, shoaling will occur when winds are too weak to produce enough vertical shear to overcome stratification at the bottom of the mixed layer. Upwelling is a coastal, spring-summer phenomenon and seasonal warming peaks in late summer or early fall. It should be possible to separate these effects using season- and station-specific regressions, but the results summarized in Table I-1 show that, on average, there is no gain in precision (r^2 decreases when calculated within stations and seasons).

Figure I-8 illustrates relationships at CalCOFI station

90.70, located ~300 km west of San Diego. Although the station is beyond the immediate influence of coastal upwelling, the regression of mixed layer depth on surface temperature is significant only for summer (r^2 = 0.21). Mean summer mixed layer depth is 31.2m with a standard error of 14.0m, while the rms error about the regression line is 12.6m, only 10% less than the standard error. An exceptionally large improvement is realized at station 120.90: in summer, mean mixed layer depth is 37.6 m with a standard error of 22.7m, while the regression rms error is 14.0m, an improvement of 38%. Generally, however, surface temperature does not give useful information about mixed layer depth even using regression relationships specific for each season at each station.

In contrast to mixed layer depth, thermocline strength is strongly related to surface temperature (Figs. I-5 and I-6, Table I-1), because thermocline strength is essentially the difference between the temperature of the surface layer and the relatively constant temperature of the deep layer below the seasonal thermocline. At station 90.70 (Fig. I-8), regressions for winter, spring, and summer are significant (r^2 = 0.34, 0.27, and 0.33, respectively). While mean spring surface temperature (14.55 ^{o}C) is only slightly less than mean winter surface temperature (14.69 ^{o}C), the regression intercepts are different: at the same temperature, thermocline strength in winter is 20% greater than thermocline strength in spring. This illustrates the value of season-specific regressions. In fall, regression between thermocline strength and surface temperature is not significant. Very

large thermocline gradients exist without a rise in surface temperature.

South of Point Conception and within 300-500 km of the coast, regression on surface temperature gives an estimate of thermocline strength that is 20-40% more precise than an estimate equal to the seasonal mean. For example, at station 110.70, summer thermocline strength estimated from the climatological mean is 0.109 $\pm$0.040 $^{o}C\ m^{-1}$. From an observed surface temperature of 19.0 ^{o}C (0.4 ^{o}C above the mean), one could estimate with equal confidence that the thermocline strength is 0.166 $\pm$0.029 $^{o}C\ m^{-1}$.

Thermocline strength is most strongly related to surface temperature in the Southern California Bight, in shallow coastal waters north and south of Pta. Eugenia, and in a band parallel to the coast ~200 km off Pta. Eugenia (areas within the 0.70 contour of relative rms error, Fig.I-6). Circulation in the Southern California Bight is dominated by the semi-closed Southern California Eddy. Bahia Sebastian Vizcaino, to the north of Pta. Eugenia, is likewise isolated from the large-scale flow of the California Current and Inshore Countercurrent. Thus, local forcing at the surface may have a greater effect on subsurface structure in these coastal regions. The band offshore of Pta. Eugenia is characterized by complex meanders in the core of the California Current and a recurrent anticyclonic eddy near Guadalupe Island (Lynn et al. 1982). Attenuation of the

California Current may increase the relative impact of local forcing in this region as well.

4.2. Vertical coherence of mesoscale structure

Temperature patterns at depths below the mixed layer are coherent with surface temperature patterns ($r^2 > 0.50$) in coastal, transition, and oceanic regions off central California and Pt. Conception and in coastal regions off northern Baja California and Pta. Eugenia (Table I-2). Coherence to adepth below the mixed layer occurs most frequently in regions with shallow mixed layers, but occasionally occurs in oceanic regions with deeper mixed layers. In other cases, r^2 falls below 0.50 within the mixed layer and to a value as low as 0.24 at the mixed layer depth.

Correlation is a simple way to compare surface and subsurface patterns, but may underestimate the value of surface patterns as manifestations of subsurface structure. For example, Simpson et al. (1984) used sea surface temperature imagery in a study of a three-layer eddy in the transition zone off Pt. Conception. The subsurface warm-core eddy was clearly manifested as a warm patch at the surface, but there was a cold-core layer at 75-175m between the eddy and the warm surface layer. Although the anticyclonic flow of the eddy was coherent to ~1000m, correlation with the surface temperature pattern dropped to zero in the cold-core layer (Simpson et al. 1986).

Surface-subsurface temperature correlation profiles show two basic patterns in the CalCOFI data set: (1) a monotonic decrease of r with depth or (2) a minimum r at an intermediate depth between 50 and 125m (Fig.I-7). Correlation minima occuryear-round at 50-75m in the Southern California coastal region and in spring, summer and fall at 75-125m in the Border coastal region. These correlation minima occur below the thermocline, the strength of which is very strongly related to surface temperature in the Southern California Bight. The flow of the California Undercurrent in these regions is coherent with the surface Inshore Countercurrent, but properties like temperature may be uncorrelated because the source waters of these currents are different (warm, salty equatorial Pacific water and cold, low-salinity subarctic Pacific water, respectively, Lynn and Simpson 1987). The most problematic aspect of correlation minima at intermediate depths is the increase in correlation with the surface at greater depths. A single realization of such a profile might be caused by an intrusion of a different water type at the intermediate depth, but long-term mean profiles of that shape are more difficult to explain.

Correlation minima also occur year-round at 125m in the Northern Baja California oceanic region. An offshore, secondary peak in California Current flow occurs in the upper 100-150m in this region (Lynn and Simpson 1987). Finally, correlation minima occassionally occur at 50-125m in transition regions south of Pt. Conception: Southern California and Border in fall, Northern Baja California in summer and fall, and Pta. Eugenia in winter. The

core of the California Current is found in these regions, but flow and distributions of properties in the surface layer are modified by mesoscale eddies (Lynn and Simpson 1987). Three-layer eddies, such as the one observed by Simpson et al. (1984), may be responsible for the shape of these correlation profiles.

4.3. Conclusions

Satellite imagery has proven its value in a wide range of applications, mostly limited to the surface layer of the ocean (c.f. Fiedler et al. 1984 and Marine Tech. Soc. Journal, vol. 20, no. 2, June 1986). Analysis of the CalCOFI data set demonstrates that sea surface data, as might be obtained by accurate remote sensing techniques, can provide some useful information about mesoscale structure in the surface layer above the seasonal thermocline and about the vertical structure of the water column through the thermocline.

Linear correlation analysis of the vertical coherence of mesoscale structure can only show that surface imagery provides information about thermocline fronts, subsurface eddies, or undercurrents where those features are coherent with surface layer fronts, eddies or currents. The value of surface imagery used in this way requires prior knowledge based on surface and subsurface sampling. The California Current is a relatively well-known system; great care must be taken when using remote sensing data to infer subsurface structure in less well known systems.

In the California Current, surface temperature provides some limited information about vertical thermal structure and subsurface mesoscale structure. Errors introduced into the temperature signal at the sea surface, in the atmosphere, and on board the satellite will further limit the utility of the data. In the future, measurements of sea surface winds from satellite scatterometers or ocean color from new color sensors may offer information complementary to sea surface temperature that would improve the precision of derived estimates of vertical structure parameters. Satellite sensors will be fully exploited for global, regional, and mesoscale studies of the marine environment when subsurface information can be reliably derived from satellite data.

Acknowledgements. I thank L. Eber for providing the data tape summarizing the efforts of hundreds of scientists, technicians, students, and crew during 35 years of the CalCOFI program. R. Lynn, K. Richter, and J. Simpson made comments on early drafts of the manuscript. This study was supported by an Office of Naval Technology Postdoctoral Fellowship.

REFERENCES

Bernstein, R. L., L. Breaker, and R. H. Whritner, California Current eddy formation: ship, air, and satellite results, Science, 195, 353-359, 1977.

Dugan, J. P., Characteristics of surface temperature structure and subsurface mesoscale features, Rem. Sens. Env., 9, 109-113, 1980.

Fiedler, P. F., G. B. Smith, and R. M. Laurs, Fisheries applications of satellite data in the eastern North Pacific, Mar. Fish. Rev., 46(3), 1-13, 1984.

Flament, P., L. Armi, and L. Washburn, The evolving structure of an upwelling filament, J. Geophys. Res., 90, 11,765-11,778, 1985.

Koblinsky, C. J., J. J. Simpson, and T. D. Dickey, An offshore eddy in the California Current System, Part II: Surface manifestation, Prog. Oceanogr., 13, 51-69, 1984.

Legeckis, R., A survey of worldwide sea surface temperature fronts detected by environmental satellites, J. Geophys. Res., 83, 4501-4522, 1978.

Lynn, R. J., K. A. Bliss, and L. E. Eber, Vertical and horizontal distributions of seasonal mean temperature, salinity, sigma-t, stability, dynamic height, oxygen and oxygen saturation in the California Current, 1950-1978, CalCOFI Atlas No. 30, 513 pp., University of California, San Diego, 1982.

_____, and J. J. Simpson, California Current System - the seasonal variability of its physical characteristics, J. Geophys. Res., C12, 12,947-12,966, 1987.

Simpson, J. J., T. D. Dickey, and C. J. Koblinsky, An offshore eddy in the California Current System, Part I: Interior dynamics, Prog. Oceanogr., 13, 5-49, 1984.

_____, C. J. Koblinsky, J. Pelaez, L. R. Haury, and D. Wiesenhahn, Temperature - plant pigment - optical relations in a recurrent offshore mesoscale eddy near Pt. Conception, California, J. Geophys. Res., 91, 12,919-12,936, 1986.

Sokal, R. R., and F. J. Rohlf, Biometry, 776 pp., W. H. Freeman, San Francisco, 1969.

Wyllie, J. G., Geostrophic flow of the California Current at the surface and at 200 meters, CalCOFI Atlas No. 4, 300 pp., State of Calif. Mar. Res. Comm., La Jolla, 1966.

Wyrtki, K., Oceanographic Atlas of the International Indian Ocean Expedition, 531 pp., U. S. Govt. Print. Off., Washington, 1971.

_____, L. Magaard, and J. Hager, Eddy energy in the oceans, J. Geophys. Res., 81, 2641-2646, 1976.

Table I-1. R^2 values for linear regressions on surface temperature.

	Mixed layer depth	Thermocline strength
Overall	0.024	0.200
Within stations	0.153	0.267
Within stations and seasons	0.005	0.102

Table I-2. Temperature decorrelation depth (depth at which r^2=0.50 between surface temperature and temperature at depth) over the mixed layer depth by region (Fig. 1) and season. P (r^2=0.50 at mixed layer depth): + P<.05, ++ P<.01, +++ P<.001, + means decorrelation depth is deeper than mixed layer depth, - means decorrelation depth is more shallow than mixed layer depth.

		Winter	Spring	Summer	Fall
Central California	Coastal	32--	51+	21+++	35+++
		41	26	14	19
	Transition	55	79+	45+++	35
		47	44	24	27
	Oceanic	114+	251	111++	107+
		59	65	30	33
Point Conception	Coastal	27---	30	30+++	27++
		36	27	18	22
	Transition	130++	71++	49	38+
		48	48	29	30
Southern California	Coastal	30	20---	15+	16
		31	24	14	16
	Transition	64	67	44++	32
		53	55	34	31
	Oceanic	158++	74	34-	38
		70	73	46	41
Border	Coastal	32	14---	11	16
		30	17	11	15
	Transition	46	44	18---	23---
		48	47	25	29
Northern Baja California	Coastal	47++	46+++	34+++	30+++
		35	26	15	18
	Transition	55	45--	24---	32
		56	58	31	31
	Oceanic	54---	75	31	37
		66	68	36	36
Punta Eugenia	Coastal	46+++	41+++	18+++	29+++
		33	24	13	16
	Transition	44--	72++	25+	24
		49	49	22	25

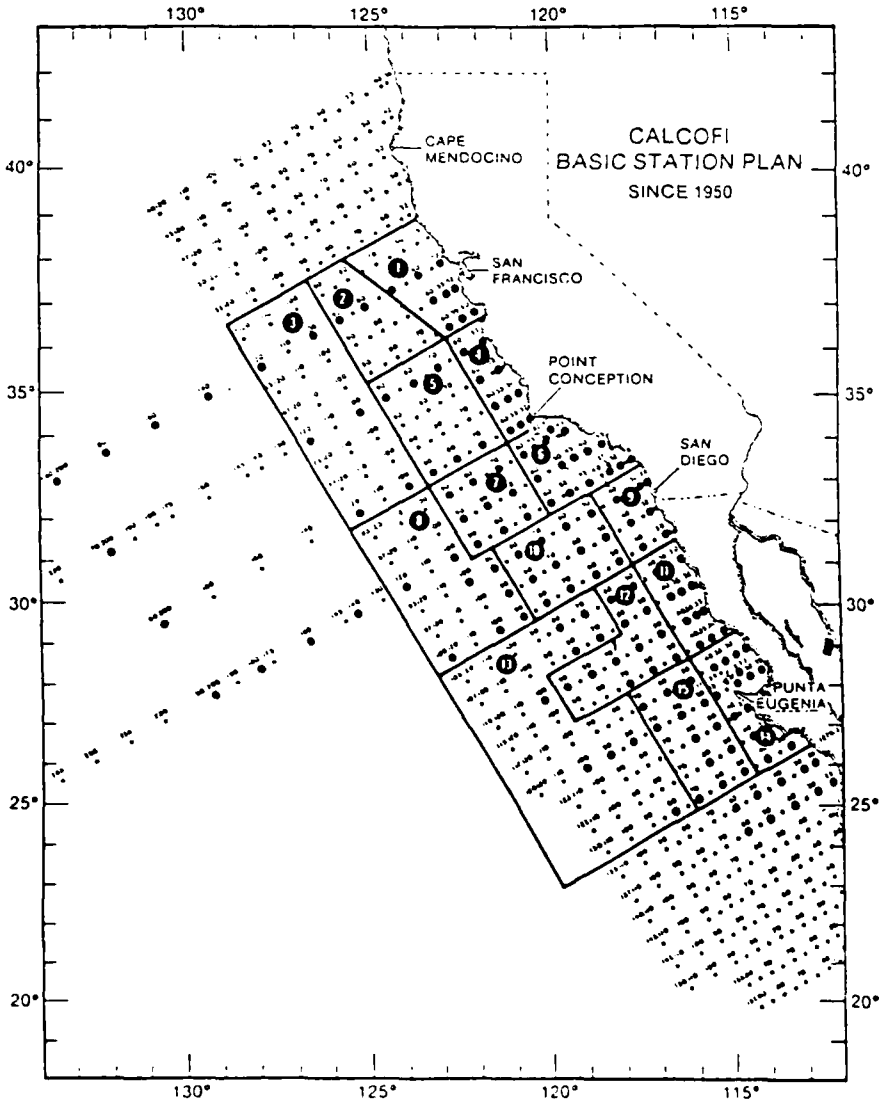

FigureI-1. CalCOFI station grid. Only the mostfrequently sampled stations (large dots) on cardinal lines 60, 70, 80, 90, 100, 110, 120, and 130, out to station 120, were used in the verical structure analysis. Regions for the correlation analysis are named as follows: Central California Coastal (1), Transition (2), and Oceanic (3); Point Conception Coastal (4) and Transition (5); Southern California Coastal (6), Transition (7), and Oceanic (8); Border Coastal (9) and Transition (10); Northern Baja California Coastal (11), Transition (12), and Oceanic (13); Punta Eugenia Coastal (14) and Transition (15).

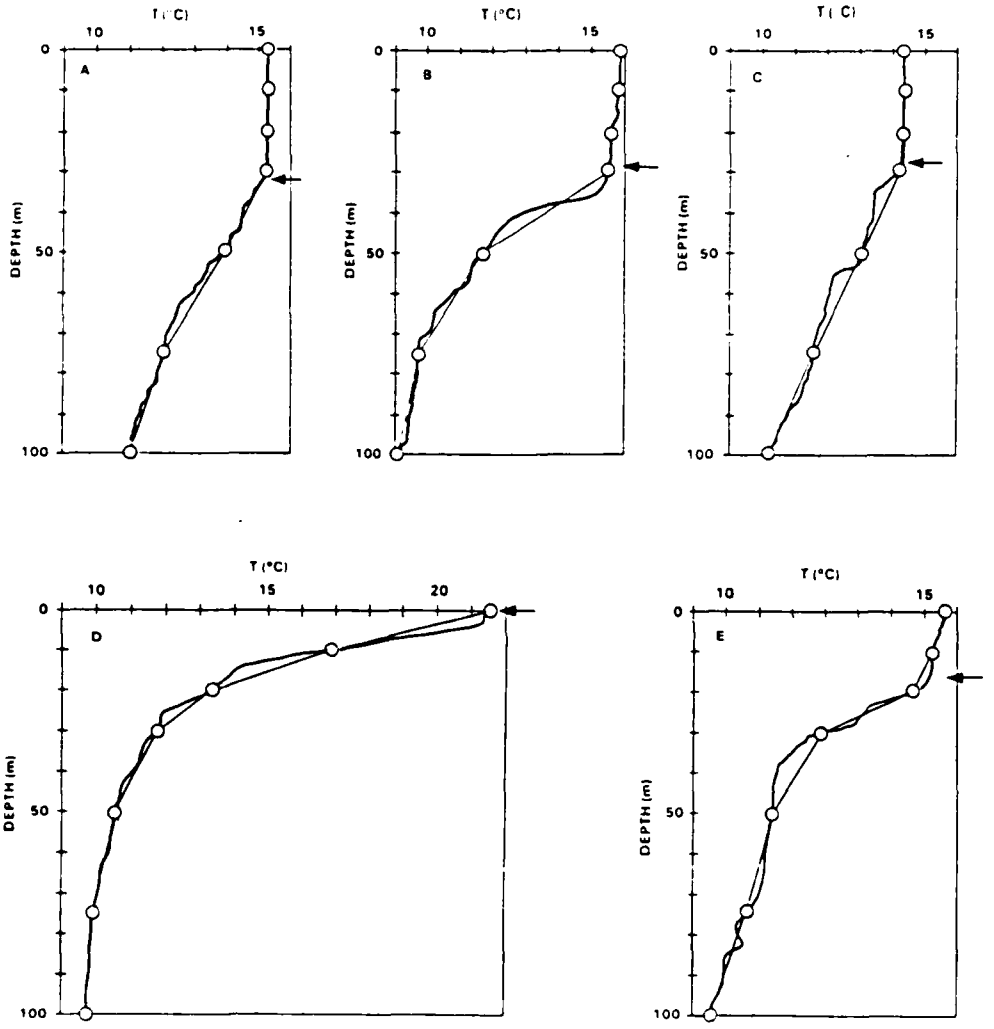

Figure I-2. A variety of CTD temperature profiles from the SouthernCalifornia Coastal region (Fig.I-1) compared to the profiles that would be observed with standard CalCOFI bottle samples at 0, 10, 20, 30, 50, 75, and 100m. Mixed layer depths (arrows) are calculated from the discrete profiles as described in the text. CTD data provided by R. Lynn.

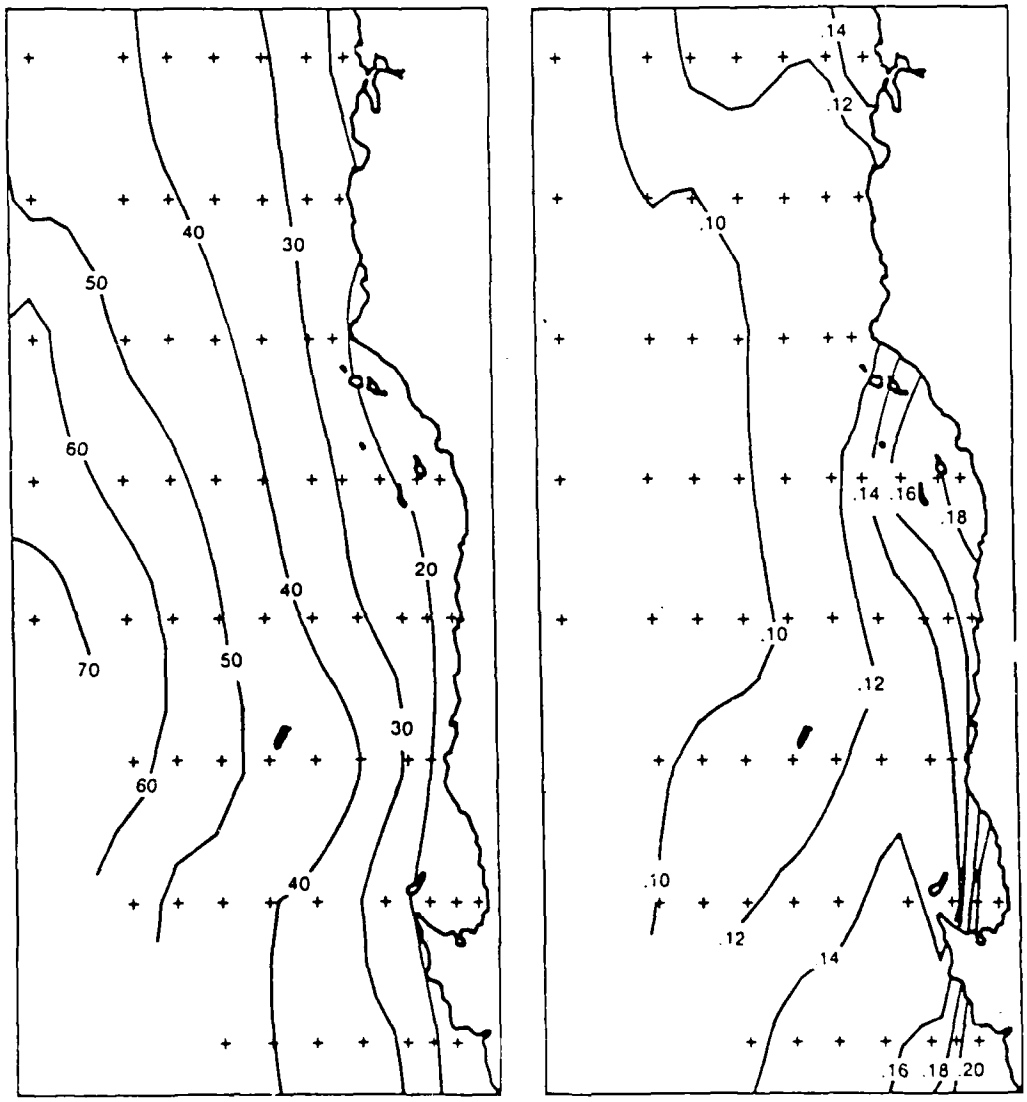

FigureI-3. Mean mixed layer depth (m) and thermoclinestrength ($^{o}C\ m^{-1}$) at 68 CalCOFI cardinal stations off California and Baja California, 1950-1984.

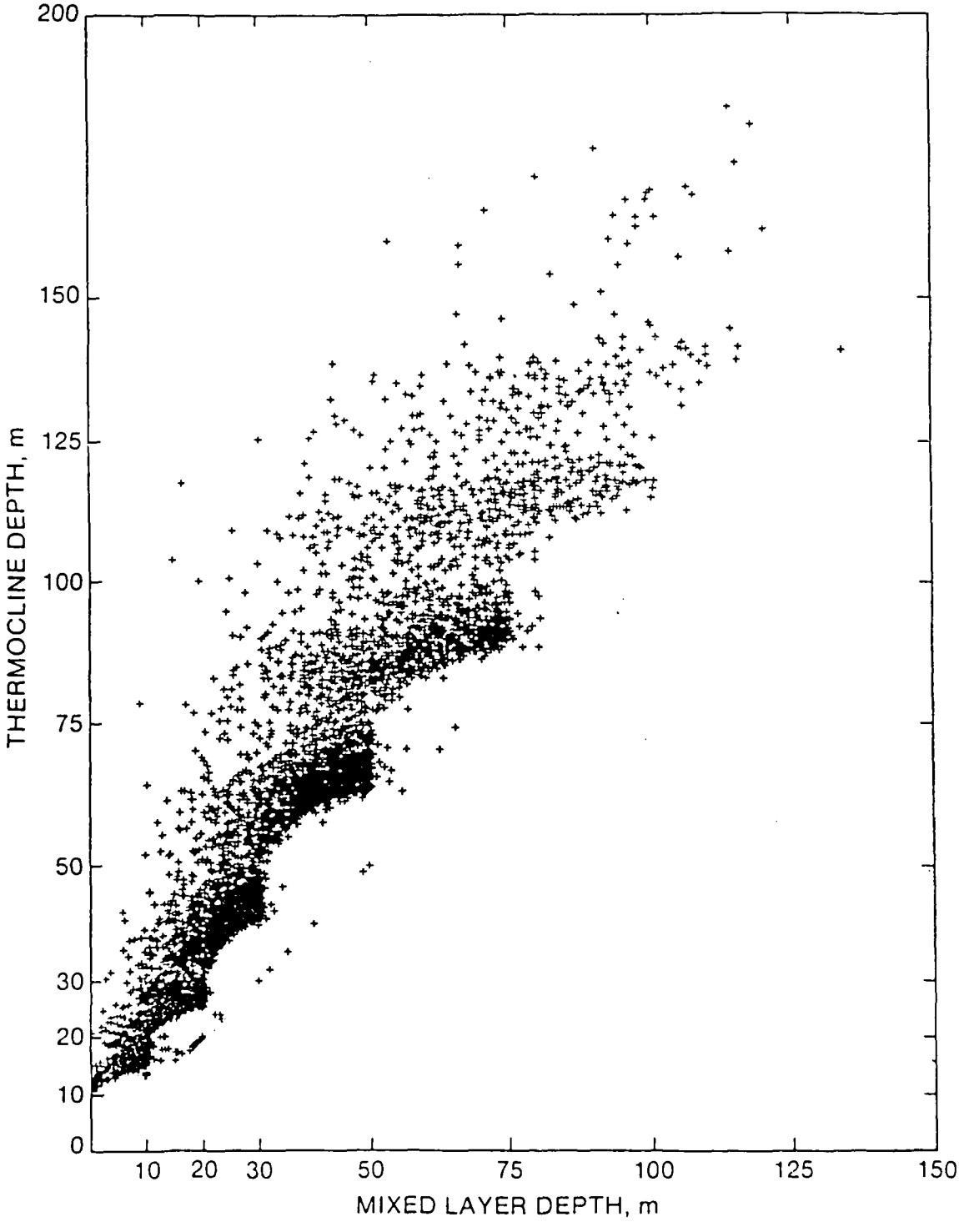

Figure I-4. Thermocline depth vs.mixed layer depth at 68 CalCOFI cardinal stations, 1950-1984.

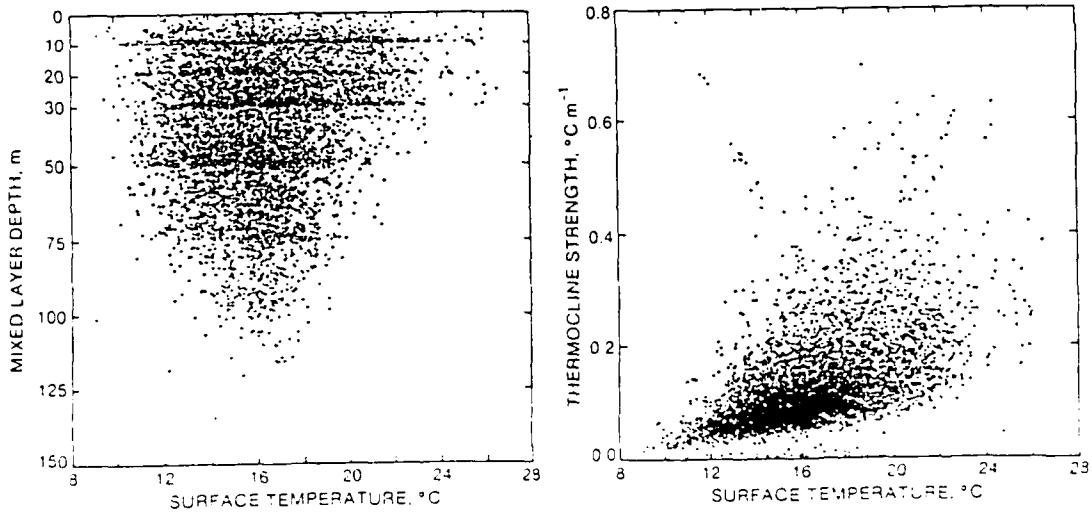

Figure I-5. Mixed layer depth vs. surface temperature (left) and thermocline strength vs. surface temperature (right) at 68 CalCOFI cardinal stations, 1950-1968.

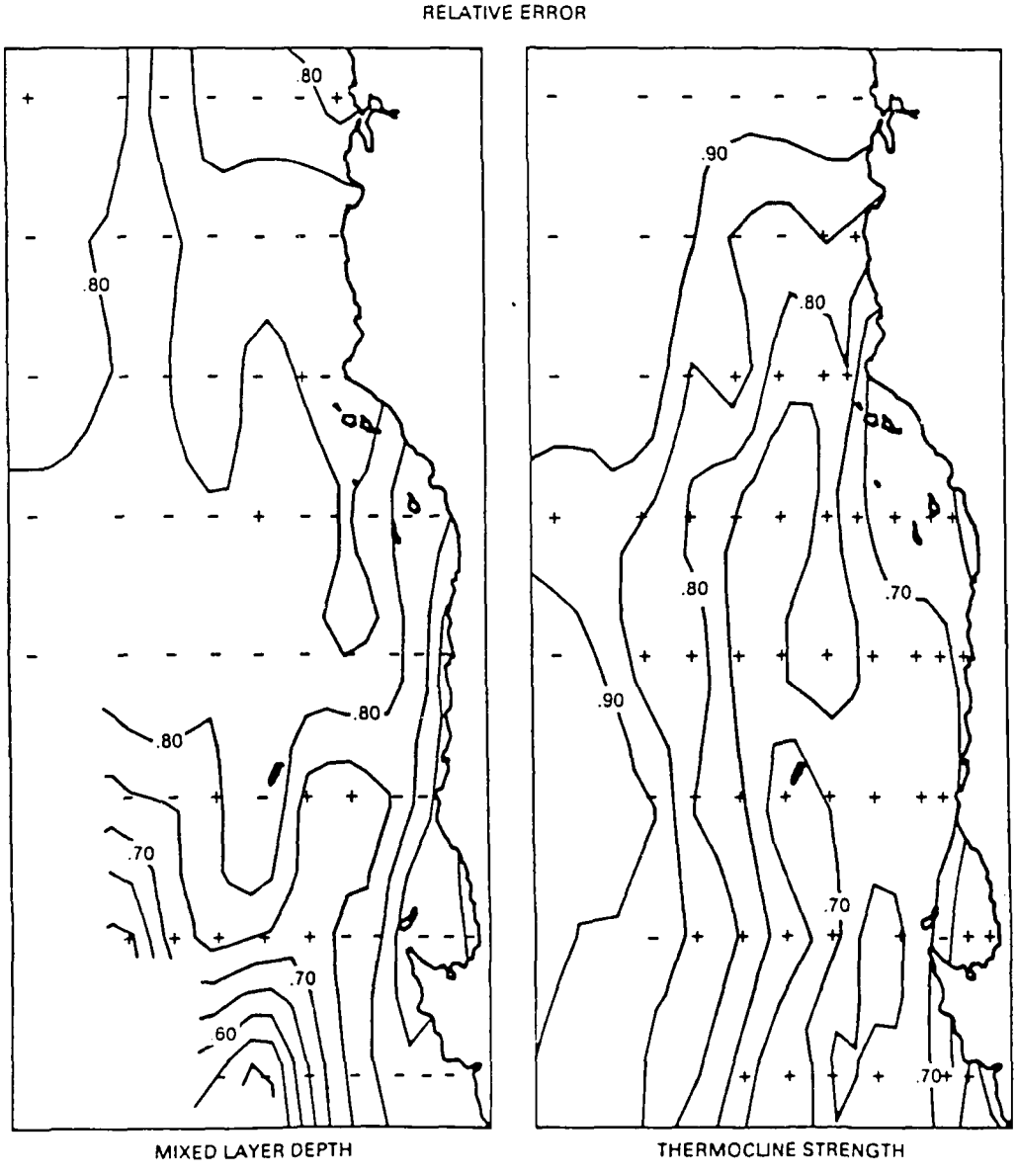

Figure I-6. Relative rms error of estimates of mixed layerdepth and thermocline strength from regression on surface temperature (+) or from the seasonal station mean (-, where the regression estimate is no more precise than the seasonal mean).

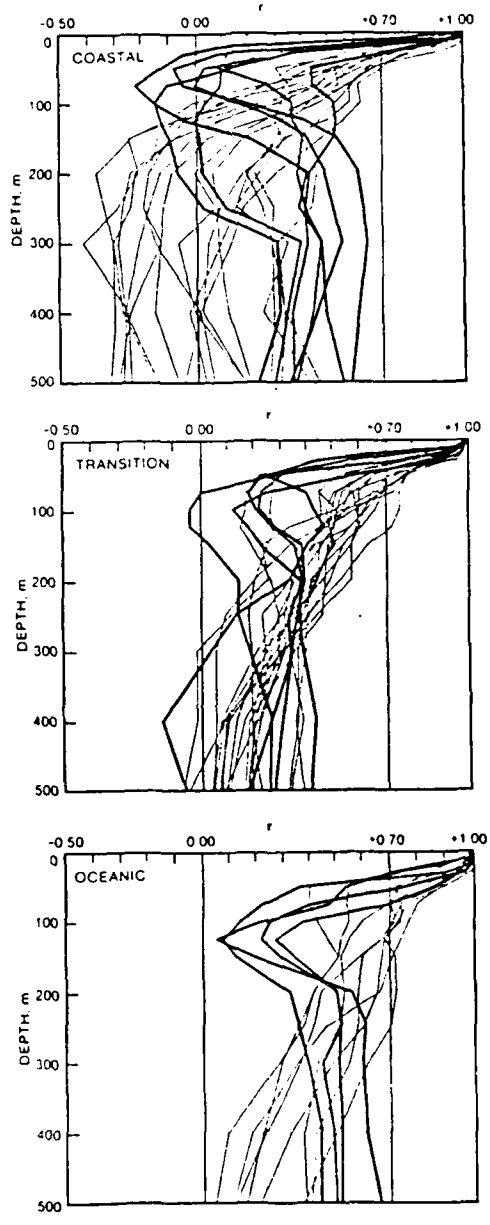

FigureI-7. Temperature correlationprofiles (correlation of surface temperature with temperature at depth, within cruises), by region and season, from 1950-1984 CalCOFI data. Heavy lines are profiles with a minumum r value that is significantly less than at least one r value at a greater depth.

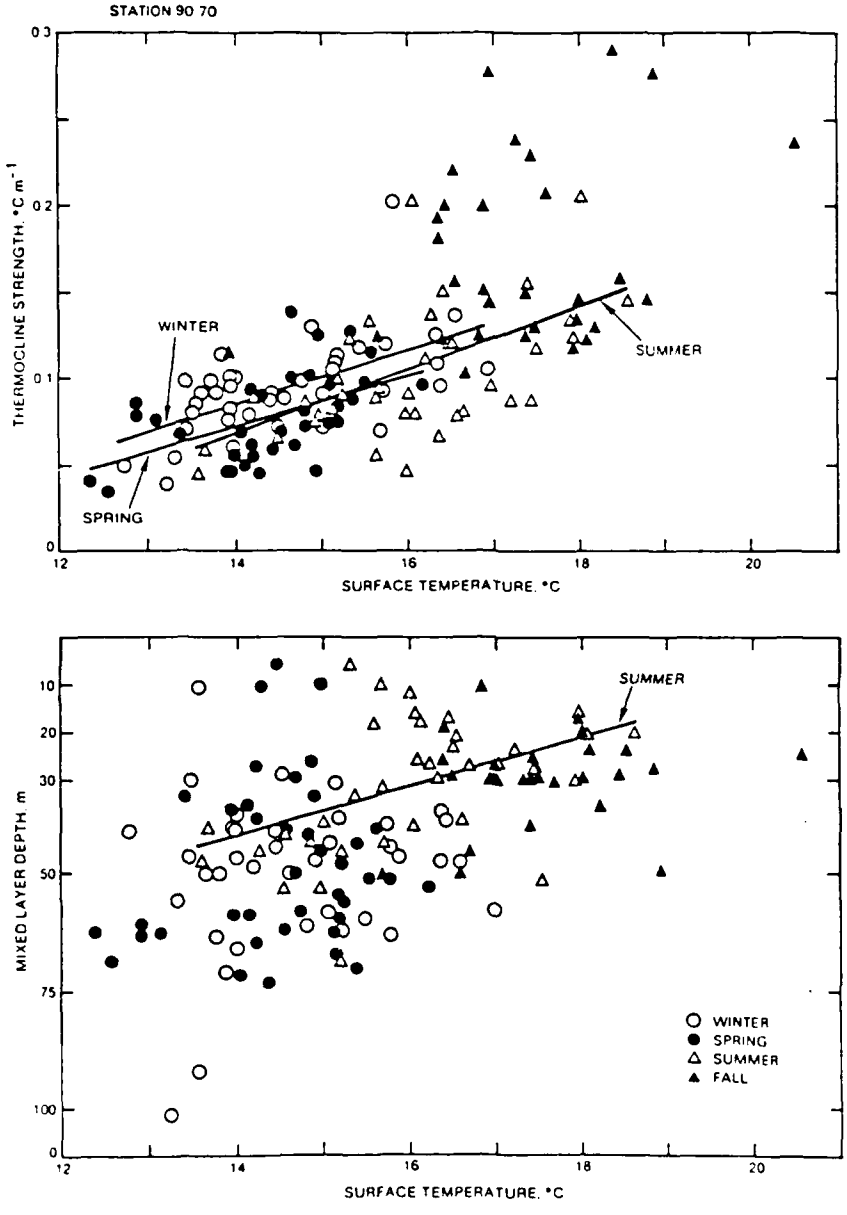

FigureI-8. Mixed layer depth vs. surface temperature (top) and thermocline strength vs. surface temperature (bottom) at CalCOFI station 90.70. Significant seasonal regression lines are indicated.

Part II. SOMAP85 - Surface Manifestations of Subsurface Thermal Structure in the Gulf of California

This study is an extension of the study described in Part I and was designed to test if (1) relationships exist between surface variables and subsurface thermal structure measured from ship and (2) such relationships can be used to derive subsurface estimates from satellite data.

Methods

A team of scientists from the Naval Ocean Systems Center (NOSC) and Centro de Investigacion Cientifica y de Educacion Superior de Ensenada (CICESE) surveyed the Gulf of California from 25 October to 4 November 1985 aboard USNS De Steiguer. Continuous underway measurements of surface temperature, chlorophyll, and pH were collected. Temperature was measured with a probe in a clean seawater intake in the bow of the ship. Chlorophyll was measured with a Turner Designs fluorometer calibrated by discrete chlorophyll extractions according to Strickland and Parsons (1972).

Expendable bathythermograph (XBT) stations are shown in Figure II-1. XBT profiles were digitized at 1-m intervals. The profiles were smoothed twice with a running mean filter (weighted 1-2-1). Then four parameters characterizing subsurface thermal structure were calculated. The mixed layer was operationally defined as the surface layer in which temperature was not more than 0.5^{o}C less than the surface temperature. Mixed layer depth

is the bottom of this layer. The thermocline was defined to include all depth intervals ≥5m in which the temperature gradient was stronger than -0.1 deg m^{-1} (calculated by central difference, depth positive downwards). Thermocline depth is the mean depth of this interval weighted by the 1-m temperature gradients. Thermocline temperature is the temperature at this depth. Thermocline gradient is the mean temperature gradient across the thermocline. An early attempt to calculate these parameters using the first and second derivatives of the temperature profiles seemed less robust when applied to complicated profiles with inversions or multiple thermoclines.

Satellite data were received, archived, and processed at the Scripps Satellite Oceanography Facility of Scripps Institution of Oceanography in La Jolla, California. Daytime thermal infrared data from channel 4 (11um) of the Advanced Very High Resolution Radiometer (AVHRR) on the NOAA-9 satellite were corrected for the effect of thin, low clouds using channel 2 (0.7-1.1um) near-infrared data (Gower 1985). Visible radiance data from the Coastal Zone Color Scanner (CZCS, on the Nimbus-7 satellite) were processed with an algorithm based on Gordon et al. (1983) to remove effects of Rayleigh and aerosol scattering and to derive pigment concentrations from corrected blue/green radiance ratios.

Surface-subsurface relationships were determined by stepwise multiple regression of each of the four thermal structure parameters on three predictor variables measured either by ship

or satellite: sea surface temperature, surface chlorophyll concentration, and the logarithm of surface chlorophyll concentration.

Results

Surface temperature and chlorophyll records are plotted in Figure II-2. Both transects are dominated by general trends of decreasing temperature and increasing chlorophyll from south to north into the Gulf. However, there are many mesoscale variations around these trends, especially in chlorophyll.

In the multiple regression analysis, sea surface temperature explains 12 to 49% of the variability of subsurface structure parameters (Table II-1). SST is a better predictor of thermocline temperature or thermocline gradient than of mixed layer or thermocline depth (Figure II-3). An additional 8 to 22% of variability is explained by surface chlorophyll and/or the log transform of surface chlorophyll. A total of 29 to 64% of subsurface structure variability can be explained by the surface variables.

Regression equations are listed in Table II-2. Regression coefficients, and even the variables that enter into the equations, vary somewhat between the two transects.

Discussion

Analysis of satellite data and subsurface structure has been delayed due to temporary inaccessibility of CZCS data at Scripps

Satellite Oceanography Facility. The results described above show that relationships exist between surface variables and subsurface structure measured from ship. The use of satellite measurements of surface variables to estimate subsurface structure in this case study will be assessed when satellite data become available.

References

Gordon, H. R., D. K. Clark, J. W. Brown, O. B. Brown, R. H. Evans and W. W. Broenkow. 1983. Phytoplankton pigment concentrations in the Middle Atlantic Bight: comparison of ship determinations and CZCS estimates. Appl. Optics 22, 20-36.

Gower, J. F. R. 1985. Reduction of the effect of clouds on satellite thermal imagery. Int. J. Remote Sensing 6, 1419-1434.

Strickland, J. D. H. and T. R. Parsons. 1972. A Practical Handbook of Seawater Analysis. Fish. Res. Bd. Canada Bull. 167, 310 pp.

Table II-1. Multiple regression r^2 values.

	SST	CHL	LOGC	Total
Mixed layer depth	.22	.06	.07	.35
Thermocline depth	.10	.05	.21	.36
Thermocline temperature	.45	.16	.01	.62
Thermocline gradient	.44	.11	-	.55

Table II-2. Multiple regression equations. MLD = mixed layer depth, TD = thermocline depth, TT = thermocline temperature, TG = thermocline gradient. aa = south-north and north-south transects combined, ab = south-north transect, ba = north-south transect.

$$MLD_{aa} = 2.63\ SST + 15.38\ CHL - 14.11\ LOGC - 59.03$$

$$MLD_{ab} = 3.88\ SST + 19.73\ CHL - 11.52\ LOGC - 91.94$$

$$MLD_{ba} = 2.56\ SST - 45.45\ CHL - 30.02$$

$$TD_{aa} = -3.76\ SST - 19.06\ CHL - 12.00\ LOGC - 143.08$$

$$TD_{ab} = -4.43\ SST - 35.12\ LOGC + 138.96$$

$$TD_{ba} = -4.48\ SST - 14.00\ LOGC + 151.29$$

$$TT_{aa} = .727\ SST + 1.54\ CHL + .712\ LOGC + 1.96$$

$$TT_{ab} = .912\ SST + 1.10\ CHL + 2.30\ LOGC - 1.70$$

$$TT_{ba} = .659\ SST + .682\ LOGC + 4.08$$

$$TG_{aa} = -.042\ SST - .118\ CHL + .934$$

$$TG_{ab} = -.040\ SST - .177\ CHL + .071\ LOGC + .955$$

$$TG_{ba} = -.059\ SST - .600\ CHL + 1.376$$

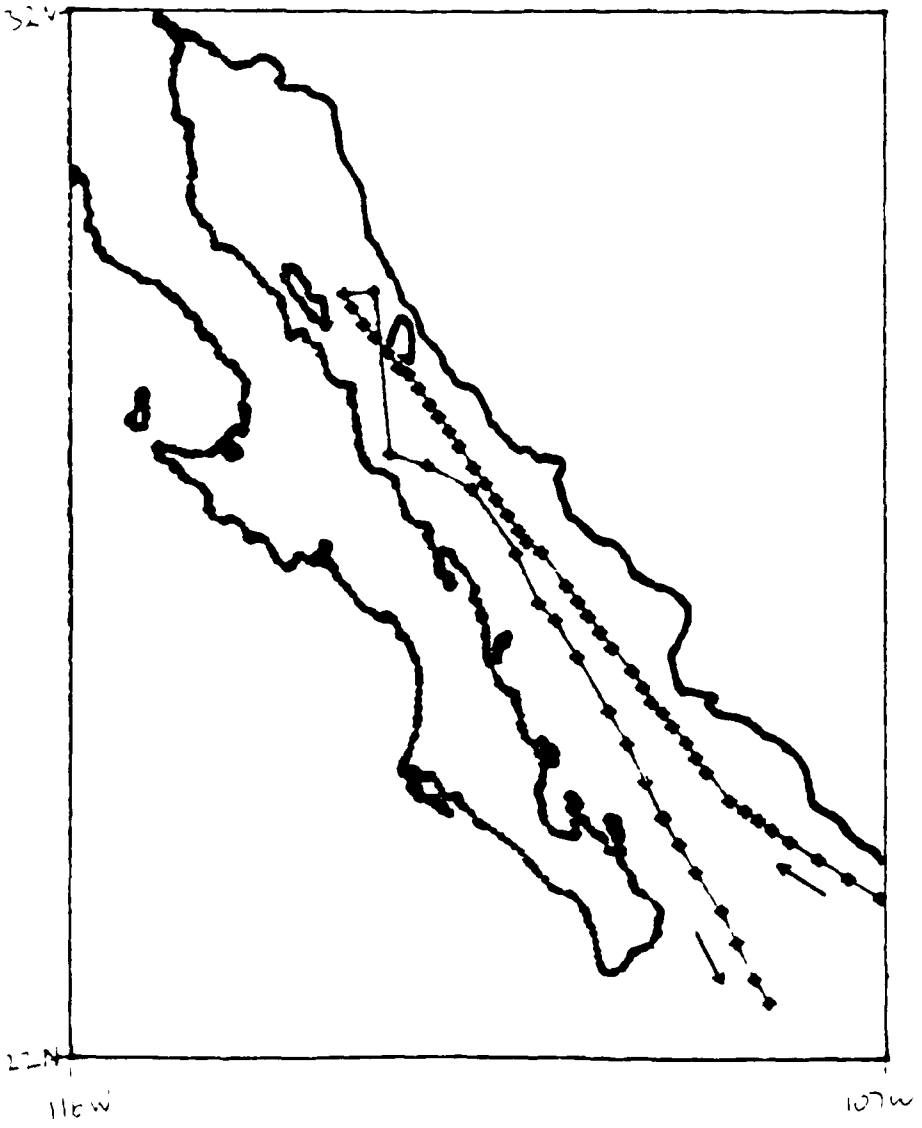

Figure II-1. XBT stations in the Gulf of California.

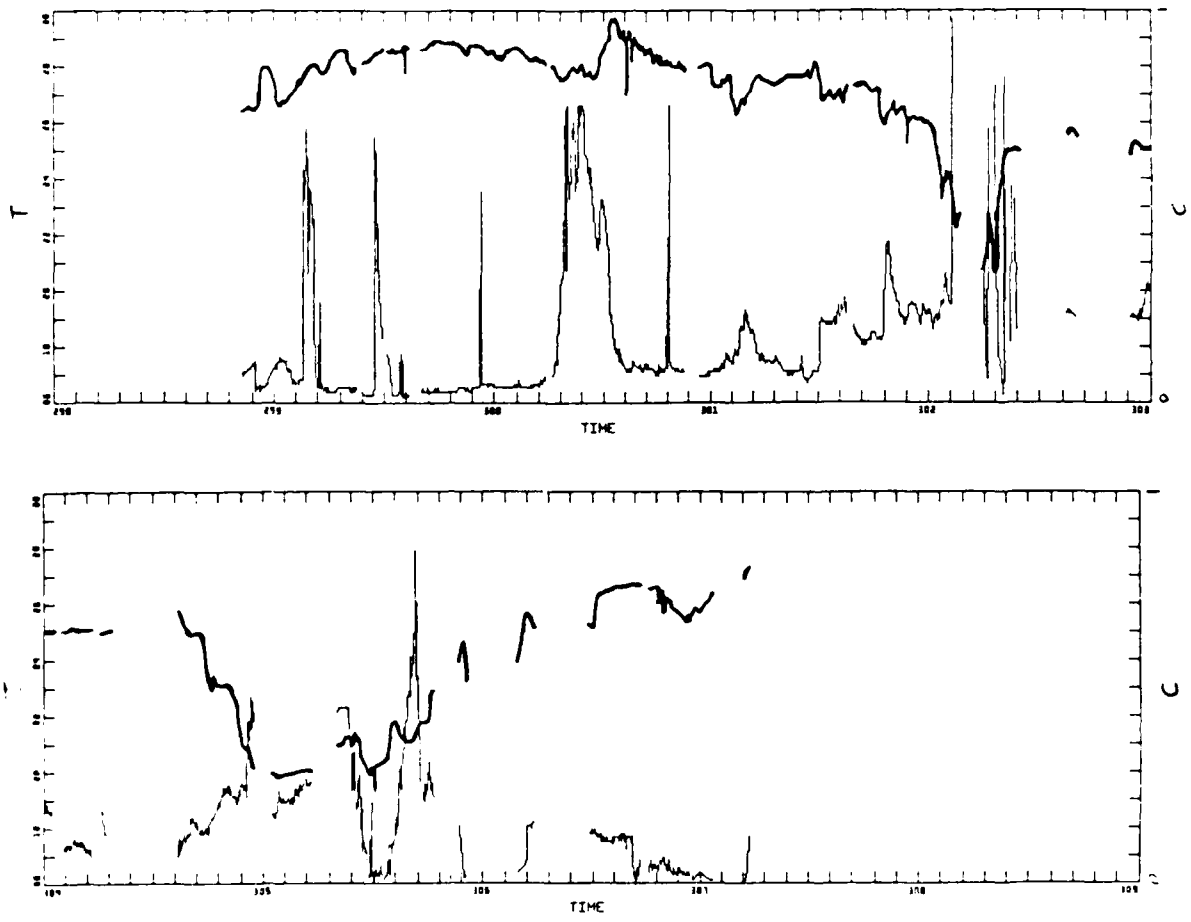

Figure II-2. Surface temperature (bold line) and chlorophyll on transects in Fig. II-1. Time in Julian days.

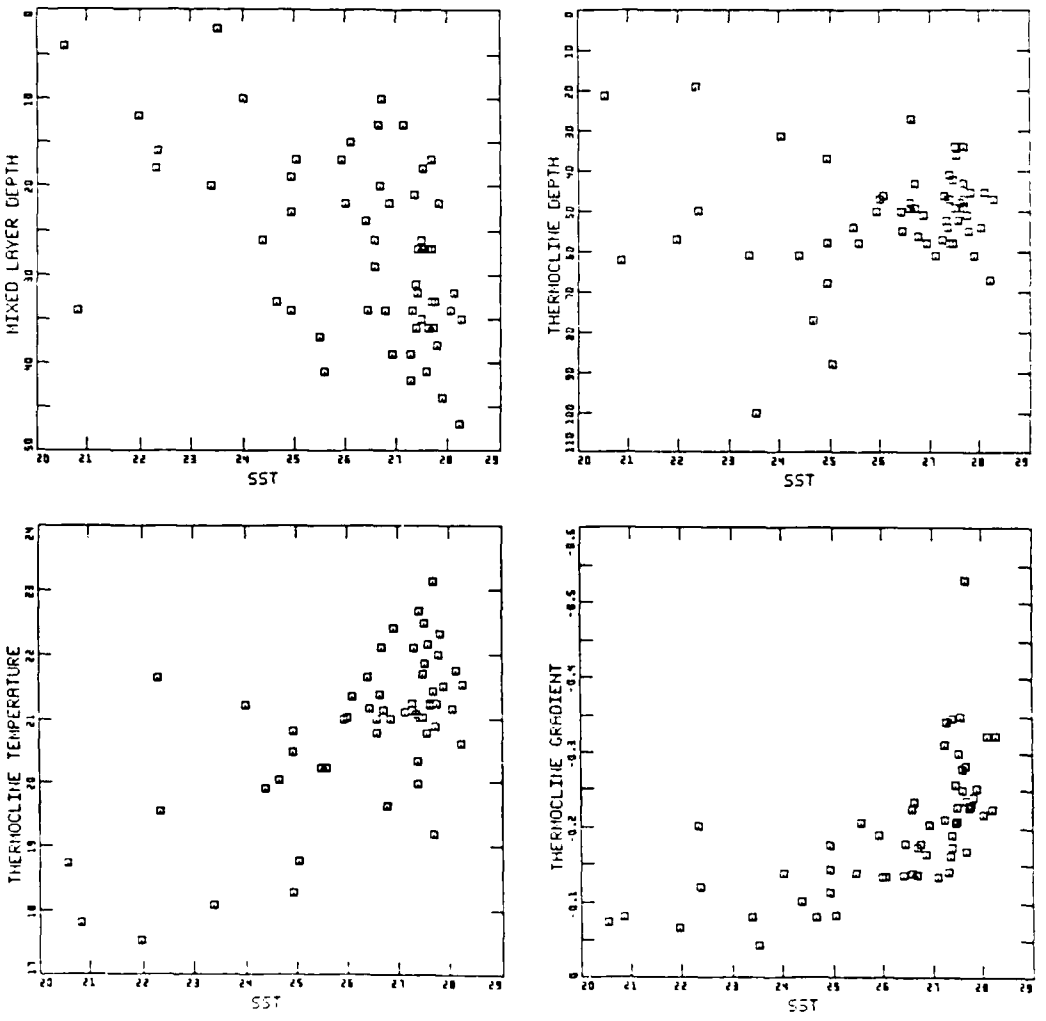

Figure II-3. Vertical structure vs. sea surface temperature (SST) at XBT stations.

Part III. A Comprehensive Vertical, Diffusive Model of the Surface Layer of the Ocean for the Personal Computer

A simple , diffusive, vertical model of the ocean surface layer was developed to investigate variations in physical forcing of vertical structure and resulting variability of surface temperature, phytoplankton biomass, and pH. The model was developed in collaboration with Dr. Robin Keir of Scripps Institution of Oceanography. It consists of a system of equations for the conservation of temperature, horizontal momentum, nitrate, phytoplankton carbon, dissolved oxygen, and total CO_2 in a vertical grid of any number of layers. In the following partial differential equations, X' means dX/dz:

Temperature

$$dT/dt = (K_d T')' + wT' + Q_s F' - Q_l$$

where $T = H/(C_{p\ o}) = H$, 10^6cal m^{-3} = cal g^{-1} = deg C

K_d = vertical eddy diffusivity, m^2 day^{-1}

$= K_v/(1 + 5Ri) + 10^{-5}$

K_v = vertical eddy viscosity, m^2 day^{-1}

$= K_o/(1 + 5Ri)^2 + 10^{-4}$

$K_o = 5 \times 10^{-3}$ $m^2 sec^{-1}$

Ri = gradient Richardson number

$= g(\ '/\ )\ /\ V'^2 = g\ \ T'/\ V'^2$

$g = 9.8$ cm sec^{-2}

= coefficient of thermal expansion

$= -0.00000875\ (T + 9)$

w = upwelling velocity, m day^{-1}

Q_s = flux of solar radiation at sea surface, 10^6cal m^{-2} day^{-1}

F = fraction of solar radiation reaching depth z

$= \exp(-k_1 z - k_2 \int_0^z P^* \, dz^*)$

k_1 = light attenuation coefficient for pure seawater

k_2 = light attenuation coefficient per unit phytoplankton

Q_l = rate of back radiation from sea surface

$= 2.172 + 0.037\ T$

Momentum

$$dV/dt = (K_v V')' + wV' - V +$$

where V = current speed, m day^{-1} = momentum per unit mass

= dissipation coefficient = 0.5×10^{-5} sec^{-1}

= surface wind stress

$= (\ _{air}/\ _{o}) C_d W^2$

C_d = drag coefficient = 1.4×10^{-3}

W = surface wind speed

Nitrate

$$dN/dt = (K_d N')' + wN' - r_N R_p P + r_N R_g \int_o^z P^* (\exp(-z^*/z_r))' \, dz^*$$

where N = nutrient nitrogen concentration, mM m^{-3}

P = phytoplankton carbon concentration, mM m^{-3}

r_N = Redfield ratio (N/C) = 0.15

R_p = phytoplankton growth rate, day^{-1}

R_g = grazing coefficient, day^{-1}

z_r = recycling depth (for $z=z_r$, $\exp(-z/z_r)=1/e$)

Phytoplankton Carbon

$$dP/dt = (K_d P')' + wP' + R_p P - R_g P$$

where R_p = phytoplankton growth rate

$= R_{max}(F \exp(1-F))\ (N/(N+K_N))$

R_{max} = phytoplankton growth constant, day^{-1}

K_N = nitrogen half-saturation concentration

Oxygen

$$dO/dt = (K_d O')' + wO' + V_O(O_{sat} - O) + r_O R_{net}$$

where O = dissolved oxygen concentration, mM m^{-3}

V_O = oxygen piston velocity at surface = 3.6 m day^{-1}

O_{sat} = saturated oxygen concentration

$= 44.655 \exp(-173.4292 + 249.6339/K + 143.3483\ln(K) - 21.8492K + S(-0.033096 + 0.014259K - 0.0017K^2)$

K = absolute temperature / 100

S = 33%

r_O = Redfield ratio (O_2/C) = 1.3

R_{net} = net carbon uptake

$= R_p P - R_g \int_0^z P^*(\exp(-z^*/z_r))'\, dz^*$

Total CO_2

$$dC/dt = (K_d C')' + wC' + V_C(C_{sat} - C) - R_{net}$$

where C = total CO_2 concentration, mM m^{-3}

V_C = CO_2 piston velocity at surface

$= 0.05 \times 3.0$ m day^{-1}

$$C_{sat} = 6442 - 537\ pH_{sat}$$

$$pH_{sat} = 8.22 - 0.01(T-20)$$

Numerical methods

The Crank-Nicholson method is used to solve the system of equations in discrete form. Time derivatives are expressed as finite differences between the present point in time, t, at which the dependent variables are known, and the next point in time, t + dt. Vertical first and second derivatives are expressed as averages of the corresponding finite differences or central differences at times t and t+dt. The resulting system of algebraic equations takes on a tridiagonal matrix form and the solution converges in one to three iterations at each time step. Oxygen and pH are not included in the iteration loop because they do not feed back on any other variables. The user specifies the number of depth intervals and total depth of the water column to be modeled, as well as the time step, in days, for solution of the discrete equations.

Formulation of the Model

Turbulent mixing is modeled as the product of the vertical gradient of a property and an eddy diffusion coefficient. Eddy diffusivity varies as a function of the gradient Richardson number (Stull and Kraus, 1987):

$$Ri = g(\ '/ \ )/V'^2$$

Here, ('/) is equal to the stability of the water column and V' is equal to velocity shear. Thus, Ri is the ratio between the

potential energy increase caused by displacement of a water parcel by turbulent motion in a stratified water column to the tubulent kinetic energy dissipated by shear. Parameterization of vertical mixing is taken from Pacanowski and Philander (1981):

$$K_v = K_o/(1 + Ri)^n + K_{vb}$$

$$K_p = K_v/(1 + Ri) + K_{pb}$$

where K_{vb} and K_{pb} are background eddy viscosity and diffusivity. Ri, the gradient Richardson number, is not allowed to go negative.

Diffusion of oxygen and carbon dioxide through the sea surface is represented by the stagnant film model (flux = piston velocity x air-sea concentration difference, where piston velocity = diffusion coefficient / thickness of the boundary layer). Piston velocities are 3.6 m day^{-1} for oxygen and 3.0 m day^{-1} for CO_2. Five percent of the CO_2 diffusing into the water is assumed to remain in the form of dissolved CO_2.

Phytoplankton productivity is a function of light and nutrients:

$$R_p = R_{max} (I/I_{max}) \exp(1-I/I_{max}) [N/(N+K_N)]$$

The model implicitly assumes that I_{max} is equal to the surface solar radiation flux, so that $I/I_{max} = F$, the fraction of surface solar radiation. The nutrient factor represents Michaelis-Menten kinetics of nutrient uptake and nutrient-limited growth.

Grazing is assumed to be a constant fraction of phytoplankton carbon per unit time. Phytoplankton grazed at

depth z^* is redistributed at depth according to $\exp(-z/z_r)$. Thus, a fraction equal to $(\exp(-z/z_r))'$ is recycled at depth z^*+z. Nitrogen and carbon are recycled immediately, utilizing oxygen.

Example model results

Figure III-1 shows time-depth plots of two runs of the model with ten 10-m layers for 200 days: low mixing, with no upwelling and 2 m sec^{-1} surface winds, and high mixing, with 0.5 m day^{-1} upwelling and 5 m sec^{-1} surface winds. Initial conditions are uniform profiles representing cold, deep water with low phytoplankton, low pH, and high nitrate concentration. Low mixing, after ten days, produces a mixed layer above a strong thermocline that continually deepens. A surface phytoplankton bloom peaks between 20 and 30 days and then declines, leaving a subsurface phytoplankton maximum, when nitrate is depleted in the mixed layer. High mixing produces a weaker thermocline which is more shallow than in the first case due to upwelling. The surface phytoplankton bloom reaches a higher peak that declines more slowly. The vertical maximum phytoplankton biomass remains at the surface.

Figure III-2 shows phytoplankton-temperature and pH-temperature plots from the two model runs. Although these plots represent covariability in time, the same relationships will be observed in the spatial domain if spatial variability is caused by asynchronous temporal cycling. Such asynchrony might be

caused by upwelling at capes and banks or by local mixing events such as storms or breaking internal waves.

The most obvious feature of both plots for both runs is the break at 11-11.5C. In this temperature range, nitrate drops to levels that significantly limit phytoplankton growth. Phytoplankton increases below this temperature and decreases above it. The negative slope of the phytoplankton-temperature plot above 11.5C is much steeper in the low mixing run because mixed layer nitrate is lower and phytoplankton growth is much less than grazing and diffusion losses.

Initial pH in these runs corresponds to oversaturation of total CO_2. Atmospheric equilibrium is never attained in either run. Phytoplankton growth accelerates the approach to equilibrium as the surface water warms. Thus, the different slopes of the pH-temperature plots above 11.5C represent the different growth rates maintained after the initial surface bloom. In the high mixing run, pH continues to increase because nutrient input by upwelling and diffusion across the thermocline are sufficient to support continued net carbon fixation by photosynthesis.

These two examples qualitatively illustrate how productivity rates, relative to the rate of heating of the surface water, are represented by the slopes of phytoplankton-temperature and pH-temperature curves. To the extent that these surface variables change through biological responses to physical mixing, they can

yield information about vertical structure of the surface water column.

References

Pacanowski, R. C. and S. G. H. Philander. 1981. Parameterization of vertical mixing in numerical models of tropicaloceans. J. Phys. Oceanogr. 11, 1443-1451.

Stull, R. B. and E. B. Kraus. 1987. The transilient model of the upper ocean. J. Geophys. Res. 92, 10745-10755.

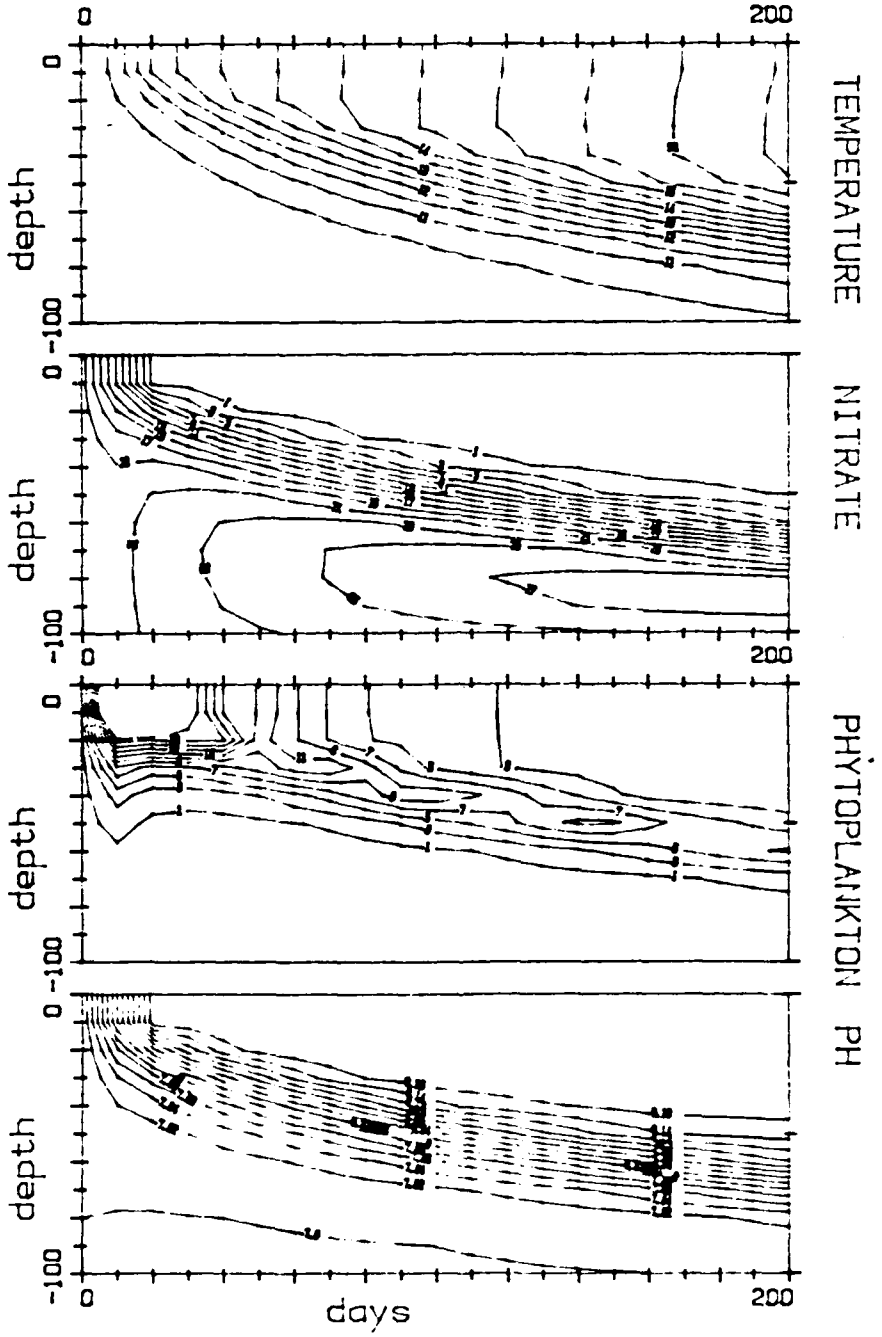

Figure III-1a. Time-depth plots of temperature, nitrate, phytoplankton carbon, and pH under low mixing conditions.

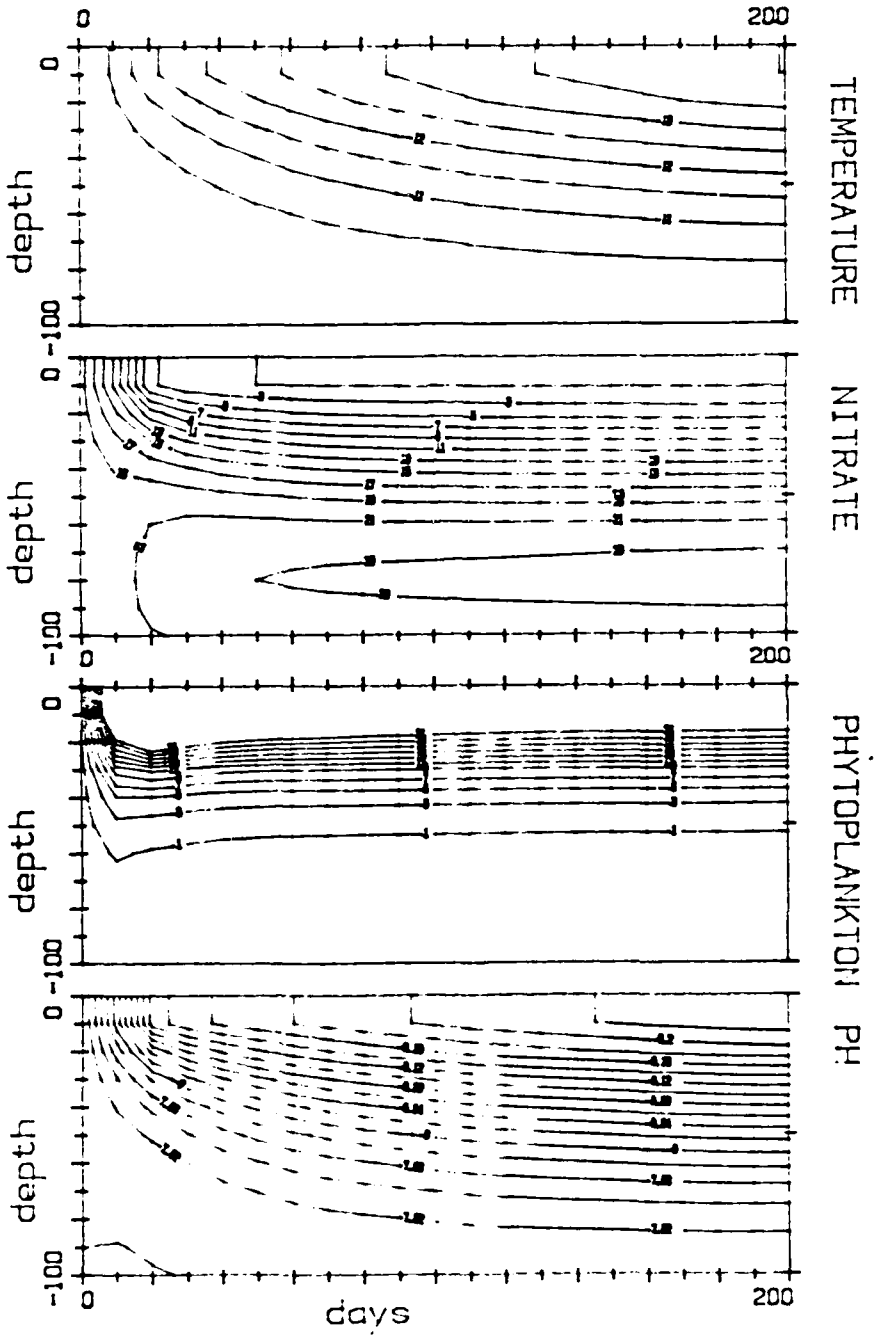

Figure III-1b. Time-depth plots of temperature, nitrate, phytoplankton carbon, and pH under high mixing conditions.

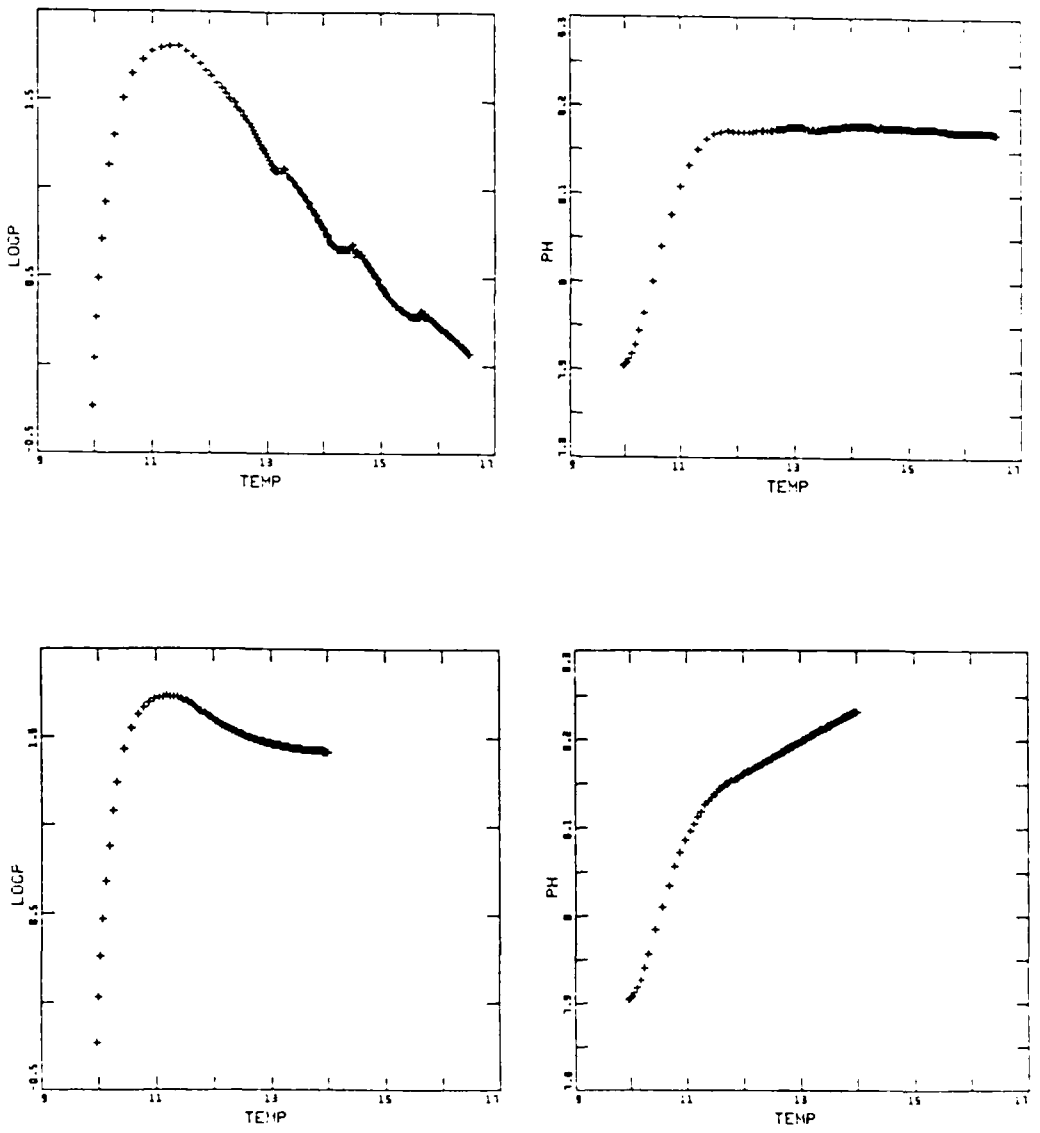

Figure III-2. Log phytoplankton carbon and pH vs. temperature, at the surface, under low mixing (top) and high mixing (bottom) conditions.

Conclusion

The analyses of historical temperature-depth data from the California Current and recent surface and XBT data from the Gulf of California have demonstrated that surface variables measurable by remote sensors do provide information about subsurface structure. However, estimates of subsurface structure based on empirical relationships are valid only regionally (coastal areas of 100's of km) and are of limited reliability, (maximum r^2 ~0.50).

A vertical model like the one developed here can be a powerful tool in studying the physical and biological mechanisms that produce empirical surface-subsurface relationships. Ultimately, such a model could serve as the basis for a scheme to maintain continuously-updated estimates of subsurface structure. The estimates would be "nowcasted" by the model using surface variables (e.g. surface temperature and color) and physical driving variables (e.g. winds, back radiation and cloudiness) monitored continuously by remote sensing.

END

DATE

FILMED

MARCH

1988

DTIC